Spontaneous Regression of Intracranial Arteriovenous Malformation on PET

Yoshio Ohmori, Masayoshi Maekawa, Yoshio Imahori, Eiji Yoshino and Satoshi Ueda
Department of Neurosurgery, Kyoto Prefectural University of Medicine, Kyoto Japan

We report a case of spontaneous regression of intracranial arteriovenous malformation (AVM) detected by PET in a 57-yr-old woman who had suffered repeated ruptures of the AVM at 28, 30 and 31 yr of age associated with pregnancy. The rupture at this hospitalization was the most critical, and after repeated ruptures for 1 mo, the AVM regressed spontaneously. The decreased cerebral blood volume (CBV) in the AVM indicated regression. The flow-to-volume (CBF/CBV) ratios surrounding the AVM increased. The metabolic rate for oxygen ($CMRO_2$) did not correlate with her improved neurological status, and an imbalance between CBF and $CMRO_2$ was recognized.

Key Words: arteriovenous malformation; spontaneous regression; PET

J Nucl Med 1996; 37:1673–1676

One of the less well-understood aspects of the natural history of intracranial arteriovenous malformations (AVM) is their potential for spontaneous regression, mostly due to the rarity of this event (*1*). There have been many reports on spontaneous regression of intracranial AVM (*2–8*) and on the hemodynamic and metabolic effects of AVM as studied by PET (*9–13*). Our goal was to document one instance of spontaneous regression in the size of intracranial AVM observed on repeat PET studies.

CASE REPORT

A 57-yr-old right-handed woman with a history of consciousness disturbance was admitted on December 14, 1992. In 1964, at the age of 28 yr, her initial clinical presentation had been a sudden headache caused by subarachnoid hemorrhage. Cerebral angiography revealed a large AVM in the right hemisphere. She was treated medically and discharged without any neurological deficits. In 1966, the then 30-yr-old pregnant woman suffered rebleeding from the AVM, which caused left hemiparesis. She had an induced abortion, was treated medically and was discharged with mild left hemiparesis. In 1967, while pregnant, she suffered a third rebleeding episode with increased severity of the left hemiparesis. She delivered and was not treated surgically; her condition gradually improved and she remained well except for slight left hemiparesis.

On this admission, CT revealed right intracerebral hematoma (6.5 × 3 × 5 cm) on the anterolateral side of the AVM, intraventricular hemorrhage and previous infarction in the right temporal lobe. We diagnosed her illness as the fourth repeated rupture of the AVM. Neurological examination confirmed stupor with a score of 10 on the Glasgow Coma Scale (GCS) and left hemiplegia. Left external ventricular drainage was performed. Cerebral angiography disclosed a high flow strio-capsulo-thalamic AVM fed by both anterior and middle cerebral arteries in the right basal ganglia and medial temporal lobe which drained into both superficial and deep veins (Fig. 1, top row) (*14*). The AVM was classed as Grade 4 according to Spetzler's grading system (*15*). We concluded that it was inoperable. During 22-day ventricular drainage, her condition improved gradually to delirium with a GCS score of 14. However she suffered minor rebleeding into the lateral ventricle causing coma, and external ventricular drainage was performed again on January 12, 1993. Two days later, the first PET study was performed while lowering the increased intracranial pressure with the ventricular drainage open.

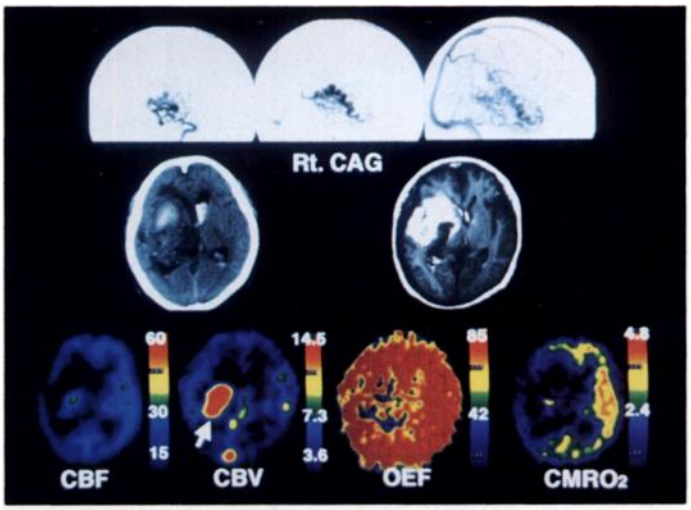

FIGURE 1. Intital PET study (obtained on Day 31 of hospitialization), CAG (top row), CT, MRI (middle row), CBF, CBV, OEF and $CMRO_2$ images (bottom row) taken at a level parallel to and 4.5 cm above the orbito-meatal line. A large proportion of the hematoma has been absorbed. Note generalized misery perfusion, hypometabolism and increased CBV in the AVM. Arrow indicates the AVM on the CBV image. Results of arterial gas analysis were: pH 7.513, $PaCO_2$ 28.1 mmHg, PaO_2 94.2 mmHg, SaO_2 97.9% and hemoglobin concentration 10.5 g/dl during inhalation of 3 liter/min of O_2 mixed air. Values described below are for normal volunteers aged 22–65 yr, mean age 45 yr. CBF values were 44 ± 7 ml/100 g/min in the cortex and 25 ± 4 ml/100 g/min in the white matter; CBV values were 4.5 ± 1.0 ml/100 g and 2.8 ± 0.7 ml/100 g, respectively. Mean CBF-to-CBV ratio was 9.8 ± 1.3 min^{-1}, and the OEF value was 44.3% ± 5.1%. The $CMRO_2$ values were 3.5 ± 0.5 ml/100 g/min in the cortex and 2.0 ± 0.3 ml/100 g/min in the white matter.

PET studies were performed on a tomograph providing an in-plane resolution of 8.6 mm (FWHM), thereby permitting simultaneous scanning of three transaxial 11–13-mm thick slices. Three planes were established 1.5 cm apart, 3.0, 4.5, and 6.0 cm above and parallel to the orbitomeatal line. We measured, in the resting state, regional cerebral blood flow (CBF), oxygen extraction fraction (OEF), and the metabolic rate for oxygen ($CMRO_2$) using ^{15}O-labeled gas steady-state technique as described by Frackowiak et al. (*16*). Regional cerebral blood volume (CBV) was measured using the bolus inhalation of ^{15}O-labeled carbon monoxide gas according to the method of Phelps et al. (*17,18*). We corrected overestimations of OEF and $CMRO_2$ by CBV according to the method of Lammertsma and Jones (*19,20*). We calculated the CBF/CBV ratio as an index of cerebral perfusion pressure (*21,22*). We set contiguous 7.74 mm-diameter round regions of interest

Received Sept. 8, 1995; revision accepted Nov. 15, 1995.
For correspondence or reprints contact: Yoshio Ohmori, MD, Department of Neurosurgery, Kyoto Prefectural University of Medicine, Kawaramachi-Hirokoji, Kamigyo, Kyoto 602, Japan.

TABLE 1
Initial PET Study Results

Region	CBF (ml/100 g/min)		CBV (ml/100 g)		CBF/CBV (1liter/min)		OEF (%)		$CMRO_2$ (ml/100 g/min)	
	R	L	R	L	R	L	R	L	R	L
Frontal lobe	14.6 ± 3.0	23.4 ± 2.1	3.38 ± 0.58	2.93 ± 0.49	4.47 ± 1.31	8.10 ± 0.91	96.0 ± 10.2	87.1 ± 4.6	1.96 ± 0.36	2.91 ± 0.27
Temporal lobe	10.8 ± 1.6	27.5 ± 0.9	5.05 ± 0.94	4.58 ± 0.86	2.15 ± 1.74	6.21 ± 1.13	84.6 ± 23.0	88.3 ± 0.9	1.30 ± 0.30	3.47 ± 0.14
Parietal lobe	14.9 ± 1.7	23.3 ± 1.5	4.82 ± 0.98	3.59 ± 0.94	3.19 ± 0.61	6.84 ± 1.41	87.7 ± 6.6	82.0 ± 7.4	1.86 ± 0.24	2.72 ± 0.24
Occipital lobe	17.8 ± 3.5	20.7 ± 1.4	3.35 ± 0.82	2.92 ± 0.42	5.48 ± 0.94	7.21 ± 0.99	90.3 ± 4.2	89.4 ± 8.0	2.28 ± 0.38	2.63 ± 0.23
AVM*	—	—	24.53 ± 8.53	—	—	—	—	—	—	—
peri-AVM cortex	14.0 ± 1.9	—	4.14 ± 1.07	—	3.57 ± 0.88	—	93.1 ± 10.1	—	1.84 ± 0.26	—
White matter	5.0 ± 1.9	12.9 ± 2.9	2.43 ± 0.56	3.50 ± 0.22	3.14 ± 1.32	7.10 ± 1.13	89.7 ± 22.7	79.9 ± 12.8	0.64 ± 0.36	1.44 ± 0.26

AVM was supplied by both anterior and middle cerebral arteries, but there was crossflow through the anterior communicating artery from the contralateral internal artery. Right MCA region except previous infarctions in the right temporal lobe was regarded as the peri-AVM cortex, which was supplied by arterial branches also feeding the AVM.

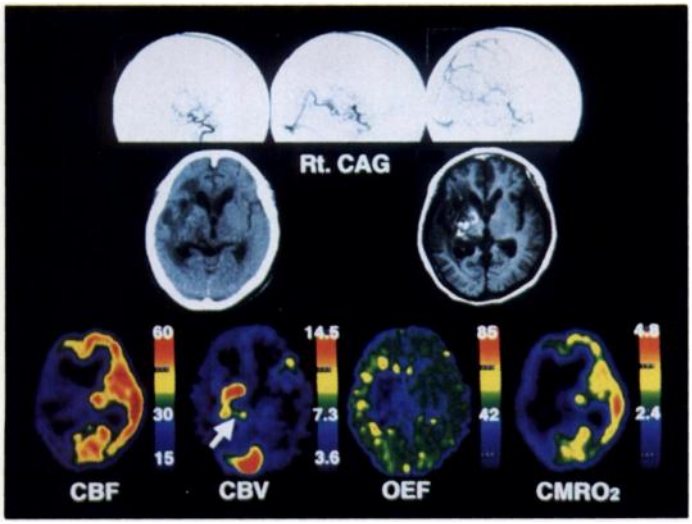

FIGURE 2. Second PET obtained 2 mo after the initial study (99th hospital day), CAG (top row), CT, MRI (middle row), CBF, CBV, OEF and $CMRO_2$ images (bottom row). Compared to the first study, total CBF was increased, the CBV in the AVM decreased, total OEF decreased,and $CMRO_2$ remained unchanged. Arrow points to regressed AVM on the CBV image. Results of arterial gas analysis were pH 7.437, $PaCO_2$ 40.1 mmHg, PaO_2 83.1 mmHg, SaO_2 96.5% and hemoglobin concentration 12.4 g/dl in room air.

(ROIs) (47 pixels) in the cortical gray matter and 6.08 mm-diameter round ROIs (29 pixels) in the white matter and basal ganglia, excluding the previous cerebral infarctions depicted on CT. No values within the AVM except CBV values are reported.

The initial PET study disclosed misery perfusion and hypometabolism throughout the whole cerebrum, particularly in the right hemisphere. On the CBV image, the AVM was demonstrated as a large vascular pool (Fig. 1 bottom row, Table 1). The OEF value was near its upper limit. Her condition improved gradually, and in February she became alert again and could take food orally. No hydrocephalus occurred. On March 23, a follow-up PET study was performed (Fig. 2 bottom row). On the CBV image, the vascular pool was decreased markedly from 24.53 to 7.81 ml/100 g, indicating decrease in the AVM size. Generalized CBF increased by 16% to 66%, the CBF-to-CBV ratios increased by 28% to 80% and the OEF decreased by 37% to 47%. The $CMRO_2$ values in the peri-AVM cortex decreased to 1.51 ml/100 g/min, which was 82% of the first value (Table 2). CBF, CBV, OEF and CBF-to-CBV but not $CMRO_2$ were improved and the improvement was compatible with her neurological recovery. Despite the improvement, the PET data still indicated both misery perfusion and low metabolism. Follow-up angiography disclosed ~70%–~80% regression of the AVM (Fig. 2, top row). MRI demonstrated thrombosed AVM (Fig. 2, middle row). The AVM was presumed to have spontaneously

TABLE 2
Second PET Study Results

Region	CBF (ml/100 g/min)		CBV (ml/100 g)	
	R	L	R	L
Frontal lobe	19.1 ± 5.4 (+31%)	34.2 ± 4.9 (+46%)	3.21 ± 0.75 (−5%)	3.37 ± 1.10 (+15%)
Temporal lobe	13.1 ± 2.9 (+21%)	36.9 ± 0.8 (+34%)	3.37 ± 0.55 (−33%)	3.53 ± 0.96 (−23%)
Parietal lobe	17.3 ± 2.5 (+16%)	37.2 ± 5.8 (+60%)	3.40 ± 0.60 (−29%)	3.44 ± 0.63 (−4%)
Occipital lobe	28.7 ± 4.7 (+61%)	34.4 ± 3.7 (+66%)	4.56 ± 2.08 (+36%)	3.43 ± 0.70 (+17%)
AVM	–	–	7.81 ± 2.69 (−68%)	–
peri-AVM cortex	16.8 ± 2.4 (+20%)	–	3.35 ± 0.70 (−19%)	–
White matter	9.1 ± 1.7 (+82%)	16.8 ± 7.0 (+30%)	2.15 ± 0.66 (−12%)	1.98 ± 0.33 (−43%)

Numbers in parentheses indicate the percent change compared to the first study.

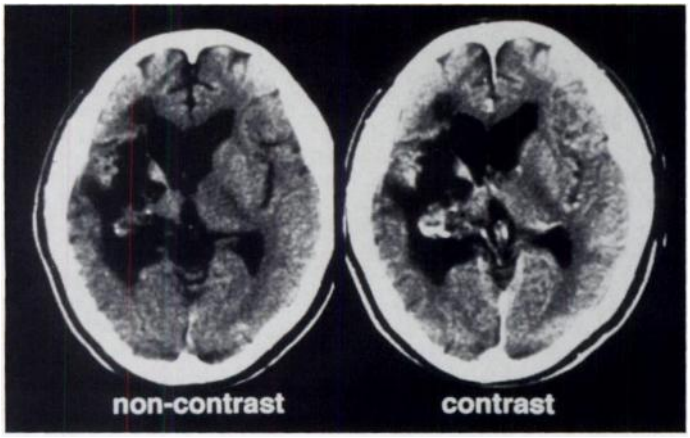

FIGURE 3. Noncontrast and contrast-enchanced CT images in 1995, 2.5 yr after the last episode of bleeding, still showed the regressed AVM.

regressed. Radiation therapy was not done for the residual AVM at the family's request. She was transferred to continue treatment in a rehabilitation program.

In 1995, 2.5 yr after the last episode of rupture, she was living at home with her family's aid, despite being moderately disabled due to left hemiparesis. CT disclosed no substantial change in the regressed but residual AVM surrounded by destroyed and absorbed brain tissue (Fig. 3).

DISCUSSION

This is a report of presumed spontaneous regression within 2 mo of intracranial AVM detected and observed by PET. The results of repeat PET studies of ruptured AVM showing spontaneous regression seem to be poorly described in the literature.

Whether any change in the AVM size occurred from 1964 to 1992 is unknown. The fourth rupture of the AVM in 1992 was the most critical, and it was followed by severe consciousness disturbance with repeated ruptures despite intensive care. Our patient's neurological status improved after the first PET study. The most common mechanism involved in spontaneous AVM regression is almost certainly that of compression of the lesion from intracerebral hemorrhage, leading to acute or subacute intravascular thrombosis (*1*).

The changes in PET parameters were attributed to both the AVM and intracranial hematoma. During the first study, hemodynamic compensatory mechanisms, such as increased OE, were seen in ipsilateral brain areas remote from the AVM and in the contralateral hemisphere. Generalized CBF was increased in both hemispheres at the second study, particularly contralaterally. The CBV values in and adjacent to the AVM decreased markedly, and the decreased CBV values were corroborated angiographically. The reduction in cerebral perfusion pressure is most reliably predicted by the CBF-to-CBV ratio (*4*). In the first PET study, the CBF-to-CBV ratios were low bilaterally but markedly increased in the second study. For each ROI in the ipsilateral hemisphere, the changes in CBV were more related to the CBF/CBV improvement *adjacent to* the AVM, whereas those in CBF were more related to that *remote from* it. The decrease in $CMRO_2$ values in the peri-AVM cortex was due to the decrease in OEF in spite of the improvement of both anemia and CBF. When hemoglobin concentration varies during repeat PET studies, CBF/CBV is a more reliable indicator than OEF, which might be greatly affected by hemoglobin concentration. Interestingly, the $CMRO_2$ values were not correlated with her neurological status since they remained at near-normal levels throughout the course due to compensatory mechanisms even in this unstable pathological condition. $CMRO_2$-CBF imbalance was recognized. Her brain after the repeated ruptures showed low perfusion and metabolism and might no longer have had normal oxygen demand, as the 1995 CT scan demonstrated atrophic change.

CONCLUSION

In this patient, hemodynamic and metabolic alteration of the apparently spontaneously regressed AVM after repeated ruptures was observed using PET. PET studies are helpful in quantifying the effects of ruptured AVM.

ACKNOWLEDGMENTS

We thank Messrs. Fujii, Horii, Wakita, Furutani and Yamagishi, Nishijin Hospital, Kyoto, Japan, for their technical assistance.

REFERENCES

1. MG Yasargil. Pathological considerations. In: Yasargil MG, ed. *Microneurosurgery 3A AVM of the brain, history, embryology, pathological considerations, hemodynamics, diagnostic studies, microsurgical anatomy.* Stuttgart: Georg Thieme Verlag; 1987:49–212.
2. Omojala MF, Fox AJ, Vinuela FV, Drake CG. Spontaneous regression of intracranial arteriovenous malformations. *J Neurosurg* 1982;57:818–822.
3. Nukui H, Miyagi O, Tamada J, Mitsukas S, Kawafuchi J. Long- term follow-up study by cerebral angiography in cases with arteriovenous malformation of the brain–with special reference to spontaneous disappearance of arteriovenous malformation in cerebral angiography-. *Neurol Med Chir (Tokyo)* 1982;22:125–132.
4. Pasqualin A, Vivenza L, Rosta R, Scienza R, Da Pian R, Colangeli M. Spontaneous disappearance of intracranial arteriovenous malformations. *Acta Neurochir* 1985;76: 50–57.
5. Takeshita M, Kagawa M, Sato K, et al. Arteriovenous malformation:3. Dynamic CT of arteriovenous malformation. *Neurol Surg (Jpn)* 1986;14:733–739.
6. Takano S, Nose T, Maki Y, Shinohara A, Kukita C. Spontaneous occlusion of a cerebral arteriovenous malformation: report of a case. *Neurol Surg (Jpn)* 1987;15: 991–996.

TABLE 2
(continued)

CBF/CBV (liter/min)		OEF (%)		CMR02 (ml/100g/min)	
R	L	R	L	R	L
6.23 ± 2.04 (+39%)	10.73 ± 2.22 (+32%)	53.5 ± 4.1 (−44%)	47.4 ± 2.4 (−46%)	1.66 ± 0.38 (−15%)	2.68 ± 0.37 (−8%)
3.88 ± 5.31 (+80%)	11.17 ± 1.82 (+80%)	53.7 ± 9.1 (−37%)	47.0 ± 2.6 (−47%)	1.15 ± 0.21 (−12%)	2.89 ± 0.17 (−17%)
5.25 ± 1.20 (+65%)	10.93 ± 1.26 (+59%)	54.2 ± 1.3 (−38%)	49.9 ± 1.8 (−39%)	1.55 ± 0.24 (−17%)	3.07 ± 0.43 (+13%)
7.01 ± 1.74 (+28%)	10.37 ± 2.01 (+44%)	52.9 ± 2.7 (−41%)	51.5 ± 3.7 (−42%)	2.50 ± 0.34 (+10%)	2.92 ± 0.24 (+11%)
–	–	–	–	–	–
5.24 ± 1.31 (+47%)	–	54.6 ± 2.5 (−41%)	–	1.51 ± 0.22 (−18%)	–
4.41 ± 0.93 (+40%)	8.24 ± 2.07 (+16%)	48.3 ± 8.5 (−46%)	46.8 ± 5.0 (−41%)	0.71 ± 0.15 (+11%)	1.32 ± 0.61 (−8%)

7. Tasaki K, Shima T, Nishida M, Yamada T, Nishida T. Spontaneous disappearance of arteriovenous malformation in angiogram–an operated case. *Jpn J Stroke* 1990;12:40–46.
8. Ezura M, Kagawa S. Spontaneous disappearance of a huge cerebral arteriovenous malformation: case report. *Neurosurgery* 1992;30:595–599.
9. Tyler JL, Leblanc R, Meyer E, et al. Hemodynamic and metabolic effects of cerebral arteriovenous malformations studied by positron emission tomography. *Stroke* 1989; 20:890–898.
10. De Reuck J, Van Aken L, Van Landegem W, Vakaet A. Positron emission tomography studies of changes in cerebral blood flow and oxygen metabolism in arteriovenous malformation of the brain. *Eur Neurol* 1989;29:294–297.
11. Sayama I, Mizuno M, Yasui N, Kanno I, Shishido F. Regional evaluation of cerebral hemodynamics and metabolism in the arterio-venous malformation using positron emission tomography. *Surgery for Cerebral Stroke (Jpn)* 1990;18:303–308.
12. Fink GR. Effects of cerebral angiomas on perifocal and remote tissue: a multivariate positron emission tomography study. *Stroke* 1992;23:1099–1105.
13. De Reuck J, De La Meilleure G, Boon P, et al. Comparison of cerebral hemodynamic and oxygen metabolic changes due to cavernous angiomas and arteriovenous malformations of the brain–a positron emission tomography study. *Acta Neurol Belg* 1994;94:239–244.
14. MG Yasargil. Special surgical considerations. In: Yasargil MG, ed. *Microneurosurgery 3B AVM of the brain, clinical considerations, surgical and special operative techniques, surgical results, nonoperated cases, cavernous and venous angiomas, neuroanesthesia.* Stuttgart: Georg Thieme Verlag; 1988:55–368.
15. Spetzler RF, Martin NA. A proposed grading system for arteriovenous malformations. *J Neurosurg* 1986;65:476–483.
16. Frackowiak RS, Lenzi GL, Jones T, Heather JD. Quantitative measurement of cerebral blood flow and oxygen metabolism in man using ^{15}O and positron emission tomography: theory, procedure and normal values. *J Comput Assist Tomogr* 1980;4: 727–736.
17. Phelps ME, Huang S-C, Hoffman EJ, Kuhl DE. Validation of tomographic measurement of cerebral blood volume with ^{11}C-labeled carboxyhemoglobin. *J Nucl Med* 1979;20:328–334.
18. Grubb RL, Raichle ME, Higgins CS, Eichling JO. Measurement of regional cerebral blood volume by emission tomography. *Ann Neurol* 1978;4:322–328.
19. Lammertsma AA, Jones T. Correction for the presence of intravascular oxygen-15 in the steady-state technique for measuring regional oxygen extraction ratio in the brain: 1. Description of the method. *J Cereb Blood Flow Metab* 1983;3:416–424.
20. Jones T, Chesler DA, Ter-Pogossian MM. The continuous inhalation of oxygen-15 for assessing regional oxygen extraction in the brain of man. *Br J Radiol* 1976;49:339–343.
21. Gibbs JN, Wise RJ, Leenders KL, Jones T. Evaluation of cerebral perfusion reserve in patients with carotid artery occlusion. *Lancet* 1984;1:310–314.
22. Gibbs JN, Wise RJ, Leenders KL, Herold S, Frackowiak RS, Jones T. Cerebral hemodynamics in occlusive carotid artery disease. *Lancet* 1985;1:933–934.

Extensive Photopenic Osteomyelitis

Patrice K. Rehm and Alan D. Aaron
Division of Nuclear Medicine, Departments of Radiology and Orthopedic Surgery, Georgetown University Hospital, Washington, D.C.

We present a case of a previously healthy child whose osteomyelitis and septic arthritis resulted in unusually extensive photopenia on bone scintigraphy. Uptake was absent in the humeral shaft and proximal epiphysis and decreased in the proximal physis. The subsequent complicated clinical course, including surgical interventions, and bone scans is described.

Key Words: bone scintigraphy; photopenic osteomyelitis; septic arthritis

J Nucl Med 1996; 37:1676–1678

CASE REPORT

The morning of hospitalization, a previously healthy 3-yr-old girl presented to her pediatrician for pain in her left upper arm. Evaluation revealed an afebrile child with mild tenderness in her upper arm and multiple healing insect bites on her extremities. Her white blood cell count was 8800 per mm^3, with 46% polymorphonuclear cells and 34% bands. The erythrocyte sedimentation rate was 6 mm/hr. Radiographs of the left humerus were normal. The patient was begun on oral penicillin and ampicillin to treat cellulitis.

Within 24 hr, the child became febrile to 105 degrees and confused, requiring hospitalization and administration of intravenous nafcillin. Over the next 12 hr, the arm became increasingly swollen and erythematous, with eventual extension to the anterior shoulder and chest wall. Numerous petechia appeared on her trunk and lower extremities. A ^{99m}Tc-HDP bone scan demonstrated extensive photopenia of the left humerus (Fig. 1).

Based on a clinical diagnosis of septic arthritis of the shoulder and osteomyelitis of the adjacent humeral metaphysis, the patient was taken emergently to the operating room for exploration and debridement. At surgery, purulent material was found within the glenohumeral joint, with the humerus being free of obvious infection. Intraoperative gram stain and cultures revealed *S. aureus*.

Intravenous nafcillin was continued, but on the fifth hospital day, the patient remained febrile necessitating surgical re-exploration. Reaccumulation of purulent material was found in the glenohumeral joint, with additional purulence within the proximal humeral metaphysis, neither being under pressure. Two days after the second surgery, radiographs revealed periosteal reaction (Fig. 2A), while bone scintigraphy again demonstrated photopenia (Figs. 2B, C).

A third bone scan on Day 18 revealed increased activity throughout most of the humerus (Figs. 2D, E). Pretreatment and multiple subsequent blood cultures as well as cardiac echo were normal. The child defervesced and was treated with intravenous gentamicin and nafcillin for 6 wk.

At 9 wk, she presented with a pathological fracture of the

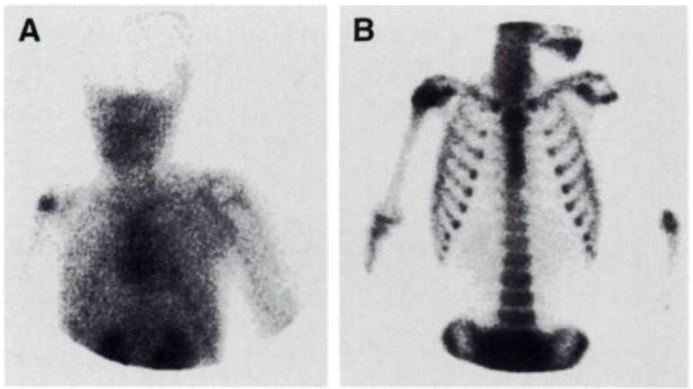

FIGURE 1. (A) Blood-pool image demonstrates relative photopenia of the left proximal epiphysis and humeral shaft, with a sleeve of increased activity around the nonvisualized shaft. (B) Delayed image demonstrates absent uptake in the entire humeral shaft and the proximal epiphysis and reduced uptake in the proximal physis. The distal metaphysis, although not optimally demonstrated, shows increased uptake.

Received May 19, 1995; revision accepted Jan. 24, 1996.
For correspondence or reprints contact: Patrice K. Rehm, MD, Division of Nuclear Medicine, Gorman 2005, Georgetown University Hospital, 3800 Reservoir Rd. NW, Washington, D.C. 20007-2113.